The EMBO Journal (2012) 31, 754–766 | © 2012 European Molecular Biology Organization | All Rights Reserved 0261-4189/12
www.embojournal.org

THE EMBO JOURNAL

ACBD3-mediated recruitment of PI4KB to picornavirus RNA replication sites

Jun Sasaki[1,3,*], Kumiko Ishikawa[1,3], Minetaro Arita[2] and Koki Taniguchi[1]

[1]Department of Virology and Parasitology, Fujita Health University School of Medicine, Aichi, Japan and [2]Department of Virology II, National Institute of Infectious Diseases, Tokyo, Japan

Phosphatidylinositol 4-kinase IIIβ (PI4KB) is a host factor required for genome RNA replication of enteroviruses, small non-enveloped viruses belonging to the family *Picornaviridae*. Here, we demonstrated that PI4KB is also essential for genome replication of another picornavirus, Aichi virus (AiV), but is recruited to the genome replication sites by a different strategy from that utilized by enteroviruses. AiV non-structural proteins, 2B, 2BC, 2C, 3A, and 3AB, interacted with a Golgi protein, acyl-coenzyme A binding domain containing 3 (ACBD3). Furthermore, we identified previously unknown interaction between ACBD3 and PI4KB, which provides a novel manner of Golgi recruitment of PI4KB. Knockdown of ACBD3 or PI4KB suppressed AiV RNA replication. The viral proteins, ACBD3, PI4KB, and phophatidylinositol-4-phosphate (PI4P) localized to the viral RNA replication sites. AiV replication and recruitment of PI4KB to the RNA replication sites were not affected by brefeldin A, in contrast to those in enterovirus infection. These results indicate that a viral protein/ACBD3/PI4KB complex is formed to synthesize PI4P at the AiV RNA replication sites and plays an essential role in viral RNA replication.

The EMBO Journal (2012) **31,** 754–766. doi:10.1038/emboj.2011.429; Published online 29 November 2011
Subject Categories: microbiology & pathogens
Keywords: ACBD3; Aichi virus; PI4KB; picornavirus; RNA replication

Introduction

All known positive-strand RNA viruses utilize intracellular membranes, such as the endoplasmic reticulum (ER), the ER-Golgi intermediate compartment, the Golgi, endosomes, or lysosomes, for genome replication. Virus infection results in remodelling of intracellular membranes, and replication complexes, where viral RNA is replicated, are formed associated with membranes. Virus-induced membrane structures are thought to increase the local concentrations of components required for replication, to provide a scaffold for anchoring the replication complexes, to prevent the activation of certain host defense mechanisms that can be triggered by dsRNA produced during virus RNA replication, and to provide certain lipids required for genome synthesis (reviewed in Miller and Krijnse-Locker, 2008).

The family *Picornaviridae* is a group of non-enveloped, single-stranded positive-sense RNA viruses. Picornaviruses include many important pathogens for humans and animals, such as poliovirus, enterovirus 71, rhinoviruses, hepatitis A virus (HAV), and foot-and-mouth disease virus (FMDV). Each genome is 7200–8500 nucleotides in length, and has a single large open reading frame (ORF) consisting of a capsid-coding P1 region, and non-structural protein-coding P2 and P3 regions. Some viruses encode a non-structural protein, leader (L) protein, upstream of the P1 region. After a large polyprotein has been translated from a single ORF, the polyprotein is processed by virus-encoded proteases into 11–12 final cleavage products. Of the non-structural proteins, 2B, 2C, and 3A, and the cleavage intermediates, 2BC and 3AB, are membrane-associated proteins (Towner *et al*, 1996; Teterina *et al*, 1997; Knox *et al*, 2005; Moffat *et al*, 2005; Krogerus *et al*, 2007), and have been reported to be involved in membrane reorganization (Cho *et al*, 1994; Aldabe *et al*, 1996; Egger *et al*, 2000; Suhy *et al*, 2000). In addition, cellular factors are thought to be required for membrane reorganization for picornavirus replication. Many studies have shown the involvement of Golgi-specific Brefeldin A (BFA) resistance factor 1 (GBF1) and ADP-rybosilation factor 1 (Arf1), which participate in the cellular secretory pathway, in the replication of enteroviruses such as poliovirus and coxsackievirus B3 (CVB3) (Belov *et al*, 2005, 2007, 2008; Lanke *et al*, 2009; Wessels *et al*, 2006a, b). Furthermore, the formation of membranous vesicles by enterovirus infection is also proposed to occur through COPII-mediated vesicle budding from the ER (Rust *et al*, 2001), or an autophagy-mediated process (Suhy *et al*, 2000; Jackson *et al*, 2005).

Recently, a model by which enteroviruses remodel membranes for viral RNA replication was proposed (Hsu *et al*, 2010). According to the model, enterovirus RNA replication begins at the Golgi/*trans*-Golgi network (TGN). Viral protein 3A anchored to membranes binds and modulates GBF1/Arf1 to enhance recruitment of phosphatidylinositol 4-kinase IIIβ (PI4KB) to the sites for viral RNA replication on the membranes, over COPI. PI4KB catalyses the production of phophatidylinositol-4-phosphate (PI4P). The produced PI4P binds to soluble viral 3D RNA polymerase and recruits it to the membranes to facilitate viral RNA synthesis. Enhanced recruitment of PI4KB on the membranes decreases anterograde transport and leads to the emergence of PI4P-enriched organelles for enteroviral RNA replication adjacent to the ER exit sites.

Aichi virus (AiV) is a member of the family *Picornaviridae* (Yamashita *et al*, 1998), and belongs to the genus *Kobuvirus*, a different genus from the genus *Enterovirus*, to which poliovirus and CVB3 belong. AiV was first isolated from patients with oyster-associated acute gastroenteritis in 1989 in Japan

*Corresponding author. Department of Virology and Parasitology, Fujita Health University School of Medicine, Dengakugakubo 1-98, Kutsukakecho, Toyoake, Aichi 470-1192, Japan. Tel.: +81 562 93 2486; Fax: +81 562 93 4008; E-mail: jsasaki@fujita-hu.ac.jp
[3]These authors contributed equally to this work

Received: 27 May 2011; accepted: 31 October 2011; published online: 29 November 2011

(Yamashita *et al*, 1991). The virus has been detected in gastroenteritis outbreaks or sporadic cases of diarrhoea not only in Japan, but also in other Asian countries, Brazil, Europe, and Africa, and is suggested to be a causative agent of gastroenteritis (Yamashita *et al*, 1995, 2000; Oh *et al*, 2006; Pham *et al*, 2007; Ambert-Balay *et al*, 2008; Goyer *et al*, 2008; Sdiri-Loulizi *et al*, 2008; Reuter *et al*, 2009; Yang *et al*, 2009). We have performed several studies to obtain an understanding of the mechanism of this virus replication, such as the characterization of some non-structural proteins and the *cis*-acting replication element at the 5′-terminus of the genome (Sasaki *et al*, 2003; Nagashima *et al*, 2005; Sasaki and Taniguchi, 2003, 2008; Ishikawa *et al*, 2010); however, the host factors involved in AiV replication remain to be elucidated.

In this study, we demonstrated that PI4KB is an essential host factor for RNA replication of AiV as in the case of enteroviruses. However, we found that AiV utilizes a different strategy to recruit PI4KB to the site of genome replication from that used by enteroviruses. We showed that AiV non-structural proteins, 2B, 2BC, 2C, 3A, and 3AB, interact with a Golgi resident protein, acyl-coenzyme A binding domain containing 3 (ACBD3). In addition, we found that ACBD3 interacts with PI4KB. No direct interaction between PI4KB and the viral proteins was detected. Knockdown of ACBD3 or PI4KB reduced virus RNA replication. Immunofluorescence microscopy revealed colocalization among the viral non-structural proteins, ACBD3, PI4KB, PI4P lipids, and dsRNA in viral RNA-replicating cells. Thus, these results indicate that a viral protein/ACBD3/PI4KB complex is formed to synthesize PI4P at the AiV RNA replication sites and plays an essential role in viral RNA replication.

Results

2B, 2BC, 2C, 3A, and 3AB interact with ACBD3

To identify host proteins involved in AiV genome replication, we searched for host proteins that interact with the AiV 2B, 2C, and 3A proteins by screening a HeLa cell cDNA library in the yeast two-hybrid system. As a result, ACBD3 was identified as a binding partner of 3A.

Using a mammalian two-hybrid system, all of the non-structural proteins including 3A were tested for binding to ACBD3. In this system, interaction between a transcription activation domain-fused protein expressed from a pACT construct and a DNA-binding domain-fused protein expressed from a pBIND construct results in transcription of the reporter firefly luciferase gene. Interaction between 3A and ACBD3 induced a 270-fold increase in luciferase activity compared with the negative control (Figure 1A). Interestingly, strong activation of luciferase expression (40- to 158-fold increase in luciferase activity) was observed also for 2B, 2BC, 2C, and 3AB.

To further confirm the interaction of these viral proteins with ACBD3, FLAG-tagged ACBD3 was co-expressed with HA-tagged L, 2B, 2BC, 2C, 3A, or 3AB in 293T cells, and then a co-immunoprecipitation assay was performed. Consistent with the results of the mammalian two-hybrid assay, 2B, 2BC, 2C, 3A, and 3AB were co-immunoprecipitated with ACBD3, but the L protein was not (Figure 1B).

Furthermore, to examine whether these viral proteins interact with ACBD3 directly, a maltose binding protein (MBP) pull-down assay was performed using glutathione S-transferase (GST)-fused ACBD3 (GST–ACBD3) and MBP-fused viral proteins (MBP–2B, MBP–2C, MBP–3A, and MBP–3AB) expressed in *Escherichia coli*. Expression of MBP-fused 2BC was not enough to use for this experiment. GST–ACBD3 was pulled down with the MBP-fused viral proteins, but not with MBP (Figure 1C).

These results indicate that 2B, 2BC, 2C, 3A, and 3AB have the ability to interact with ACBD3.

2B, 2BC, 2C, 3A, and 3AB interact with the C-terminal region of ACBD3

To determine the region in ACBD3 required for binding to the viral proteins, the ability of various deletion mutants of ACBD3 to interact with 2B, 2BC, 2C, 3A, or 3AB was investigated in the mammalian two-hybrid system (Figure 2A and B). For 2B, 2C, 3A, or 3AB, mut3 and mut5, both of which contain a C-terminal region (aa 327–528), maintained the ability to induce a greater than ∼15-fold increase in luciferase activity compared with negative controls. Also for 2BC, 7- and 4-fold increases in luciferase activity were detected with mut3 and mut5, respectively. On the other hand, mutants without the C-terminal region lacked the ability to enhance luciferase expression. These results suggest that the C-terminal region of ACBD3 is essential for binding to 2B, 2BC, 2C, 3A, and 3AB. Further detailed experiments to identify the binding domain to these viral proteins were carried out using a series of deletion mutants of mut3 (Figure 2C and D). For the five viral proteins, mut3Δ1 with the deletion of aa 328–373 enhanced luciferase expression to a similar level to mut3, but the other mutants did not. This suggests that aa 374–528 of ACBD3 are important for binding to the viral proteins.

ACBD3 colocalizes with 2B, 2C, 3A, and dsRNA in AiV RNA-transfected cells

To investigate whether ACBD3 colocalizes with viral proteins or replicating viral RNA, an AiV replicon RNA (AV-FL-Luc-5′rzm) containing a firefly luciferase gene was transfected into Vero cells by electroporation, and then an immunofluorescence assay was carried out. The replicating viral RNA was detected by staining double-stranded replicative intermediates and replicative forms using an antibody recognizing dsRNA in which the helix length is >40 bp, as carried out for other positive-stranded RNA viruses including picornavirus (Miller *et al*, 2006; Harwood *et al*, 2008; Knoops *et al*, 2008; Berger *et al*, 2009; DeWitte-Orr *et al*, 2009, Hyde *et al*, 2009). 2B, 2C, and 3A were detected as patchy clusters in the cytoplasm at 4 h after transfection (Figure 3A), and accumulated in the perinuclear region at 6 h (only the data for 3A are shown in Figure 3A). At 4 h, when viral RNA replicates actively (see Figure 5A or C), 2B, 2C, and 3A colocalized with dsRNA (Figure 3B). ACBD3, which also formed patchy clusters in the cytoplasm at 4 h after transfection, colocalized with 2B, 2C, 3A (Figure 3A), and dsRNA (Figure 3B). These results indicate that ACBD3, 2B, 2C, and 3A (and possibly also the precursor proteins 2BC and 3AB) are present in the viral RNA replication sites.

Knockdown of ACBD3 inhibits AiV RNA replication

To investigate whether ACBD3 is involved in AiV RNA replication, replication of AV-FL-Luc-5′rzm RNA was examined in Vero cells treated with small interfering RNA (siRNA) targeting ACBD3 or control siRNA. At 72 h after treatment

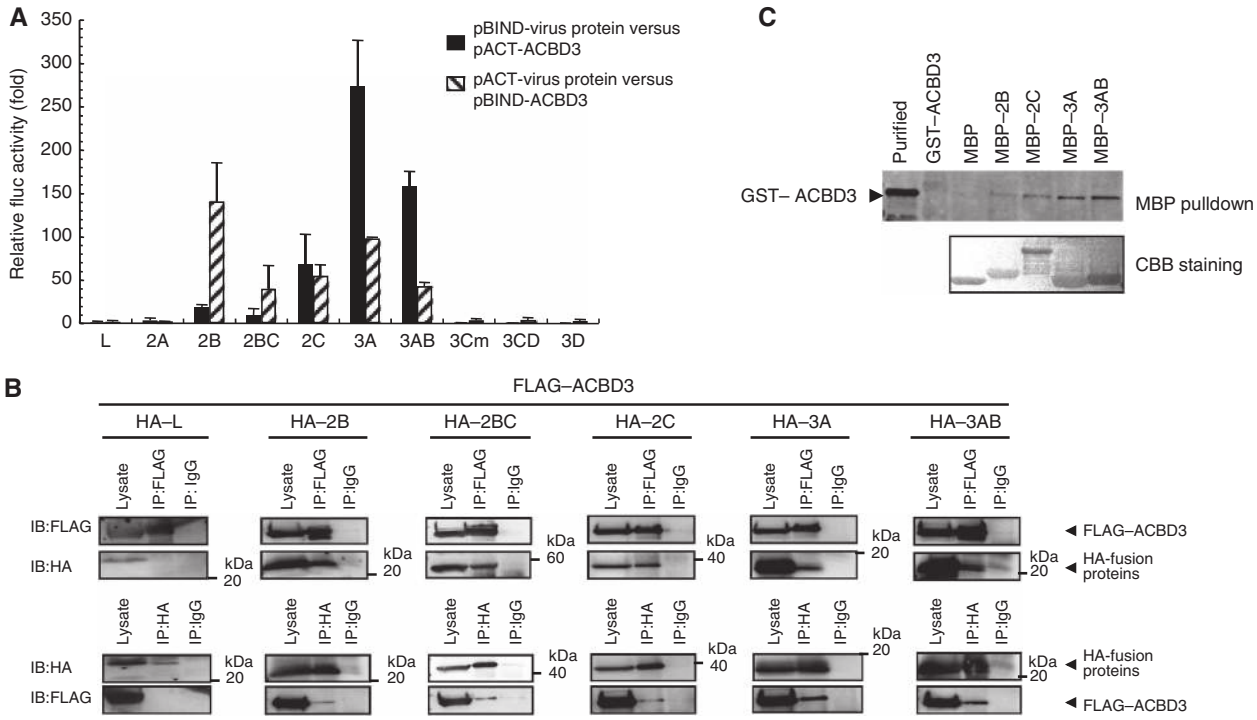

Figure 1 2B, 2BC, 2C, 3A, and 3AB interact with ACBD3. (**A**) The mammalian two-hybrid assay. The indicated combination of a pACT construct and a pBIND construct was transfected into Vero cells together with pG5luc encoding a firefly luciferase. Cell lysates were prepared at 48 h after transfection and assayed for firefly luciferase activity. Transfection efficiency was normalized by the activity of *Renilla* luciferase, which was simultaneously expressed from pBIND. The higher value of normalized luciferase activities obtained in cells transfected with the combination of the pBIND construct and empty pACT and with the combination of the pACT construct and empty pBIND was used as a negative control. The normalized firefly luciferase activity was represented as fold activation compared with a negative control. The experiment was repeated at least three times. Standard deviation bars are shown. (**B**) Co-immunoprecipitation of ACBD3 with 2B, 2BC, 2C, 3A, or 3AB. FLAG-tagged ACBD3 was co-expressed with HA-tagged L, 2B, 2BC, 2C, 3A, or 3AB. Proteins were immunoprecipitated with anti-FLAG (upper panel), anti-HA (lower panel) antibodies, or control IgG, and the resulting immunoprecipitates and whole cell lysates were analysed by immunoblotting with anti-FLAG and anti-HA antibodies. IB, immunoblotting; IP, immunoprecipitation. (**C**) MBP pull-down assay. MBP-fused viral proteins or MBP immobilized on amylose resin were mixed with purified GST–ACBD3, and proteins binding to the resin were analysed by SDS–PAGE, followed by immunoblotting with anti-GST antibody (upper panel). After immunoblotting, proteins on a PVDF membrane were stained with Coomassie brilliant blue to detect MBP-fused viral proteins or MBP (lower panel). Figure source data can be found in Supplementary data.

with siRNA targeting ACBD3, the amount of ACBD3, but not that of α-tubulin, was apparently decreased (Figure 3C). An effect of knockdown of ACBD3 on cell viability was not observed (data not shown). At 72 h after treatment with siRNA targeting ACBD3 or control siRNA, cells were transfected with AV-FL-Luc-5′rzm RNA by lipofection, and then cell lysates were prepared at various times after transfection and subjected to the luciferase assay. Knockdown of ACBD3 resulted in a decrease in luciferase activity. At 10 h after transfection, luciferase activity was decreased by ∼70% (Figure 3C). Here, Vero cells were used to exclude the effect of siRNA-induced interferon response, but a similar result was obtained using HeLa cells (data not shown). These results indicate that ACBD3 plays an important role in AiV RNA replication.

Localization of other Golgi proteins in AiV RNA-transfected cells

ACBD3 localizes to the Golgi through interaction with giantin, a Golgi protein, and the giantin-binding domain of ACBD3 has been mapped to the C-terminal region (aa 373–528) (Sohda *et al*, 2001). This region overlaps with the region important for binding to the AiV proteins (aa 374–528) (Figure 2). We then examined localization of giantin in viral RNA-replicating cells (Figure 4A). To distinguish RNA-transfected cells, a viral non-structural protein, the L protein, was immunostained. In mock-transfected cells, both ACBD3 and giantin were located in the Golgi. At 2 h after electroporation with viral RNA, the dispersion of ACBD3 and giantin was observed in some cells; however, the L protein could not be detected, because of its insufficient accumulation. At this time point, ACBD3 colocalized with giantin. As infection progressed, the redistribution of ACBD3 and giantin from the Golgi to the cytoplasm became more apparent. Importantly, at 4 h, giantin was dispersed throughout the cytoplasm, whereas ACBD3 formed clusters. As shown in Figure 3, ACBD3 colocalized with dsRNA or the viral proteins in such structures. At 4 h after electroporation, the intensity of immunofluorescence for giantin seems to be decreased compared with that in mock-transfected cells; however, no degradation of giantin was observed in an immunoblot analysis using anti-giantin antibody (data not shown).

We also examined the localization of other Golgi proteins, GM130, a *cis*-Golgi marker, and TGN46, a *trans*-Golgi marker. At 2 h after transfection with replicon RNA, dispersion of GM130 and TGN46 appears to begin like giantin, and they colocalized with ACBD3 (Figure 4B and C). GM130 was redistributed to form clusters in the cytoplasm at 4 h after transfection, but did not colocalize with ACBD3 (Figure 4B). TGN46 also became dispersed in the cytoplasm with the

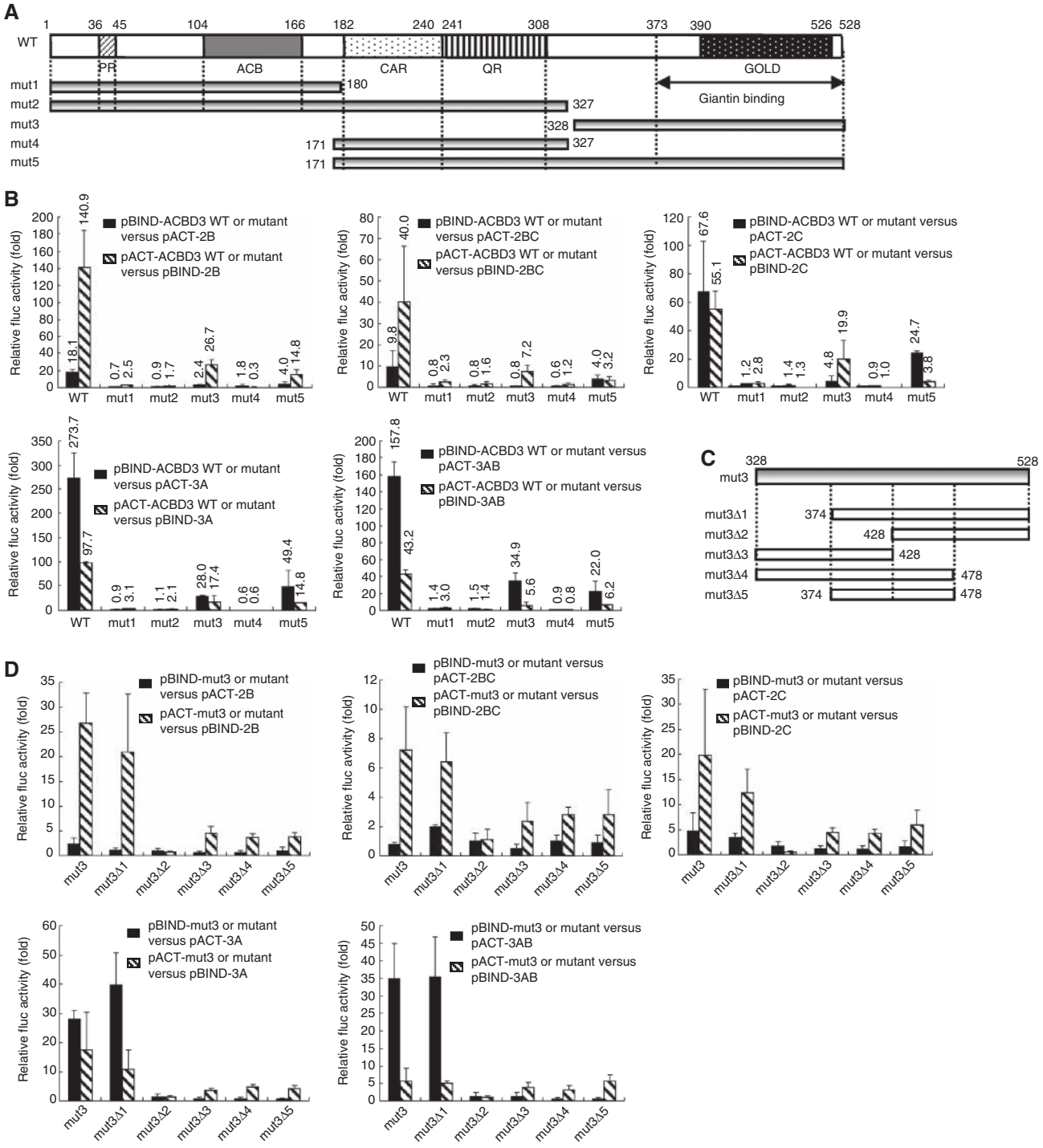

Figure 2 The C-terminal region of ACBD3 interacts with 2B, 2BC, 2C, 3A, and 3AB. (**A**, **C**) Schematic representation of (**A**) full-length ACBD3 (WT) and its mutants (mut1–mut5) and (**C**) mut3 (amino acids 328–528) and its mutants (mut3Δ1–Δ5). ACBD3 contains characteristic domains as follows: PR, proline-rich domain; ACB, ACB region; CAR, charged amino acid-rich domain; QR, glutamine-rich domain; and GOLD, Golgi dynamic domain. Numbers indicate amino-acid positions. The region between amino acids 373 and 528 is required for binding giantin. (**B**, **D**) Mammalian two-hybrid analyses were performed to examine interactions (**B**) between the ACBD3 mutants (mut1–5) and 2B, 2BC, 2C, 3A, or 3AB, and (**D**) between the mut3 mutants (mut3Δ1–Δ5) and 2B, 2BC, 2C, 3A, or 3AB, and the results are represented as described in Figure 1A. All experiments were repeated at least three times. Standard deviation bars are shown.

progression of infection, and did not colocalize with ACBD3 (Figure 4C). Thus, in viral RNA-replicating cells, other Golgi proteins examined did not colocalize with ACBD3.

AiV RNA replication requires PI4KB activity

It was recently reported that PI4KB is an essential host factor for enterovirus RNA replication (Hsu *et al*, 2010; Arita *et al*, 2011). We investigated whether PI4KB is also important for AiV replication. First, we examined the effect of a PI4KB-specific inhibitor, T-00127-HEV1 (Arita *et al*, 2011), on viral RNA replication. Vero cells were electroporated with AV-FL-Luc-5′rzm RNA, and then cultured in medium containing 0, 1, or 5 μM T-00127-HEV1. T-00127-HEV1 inhibited AiV RNA replication in a dose-dependent manner, and the replication

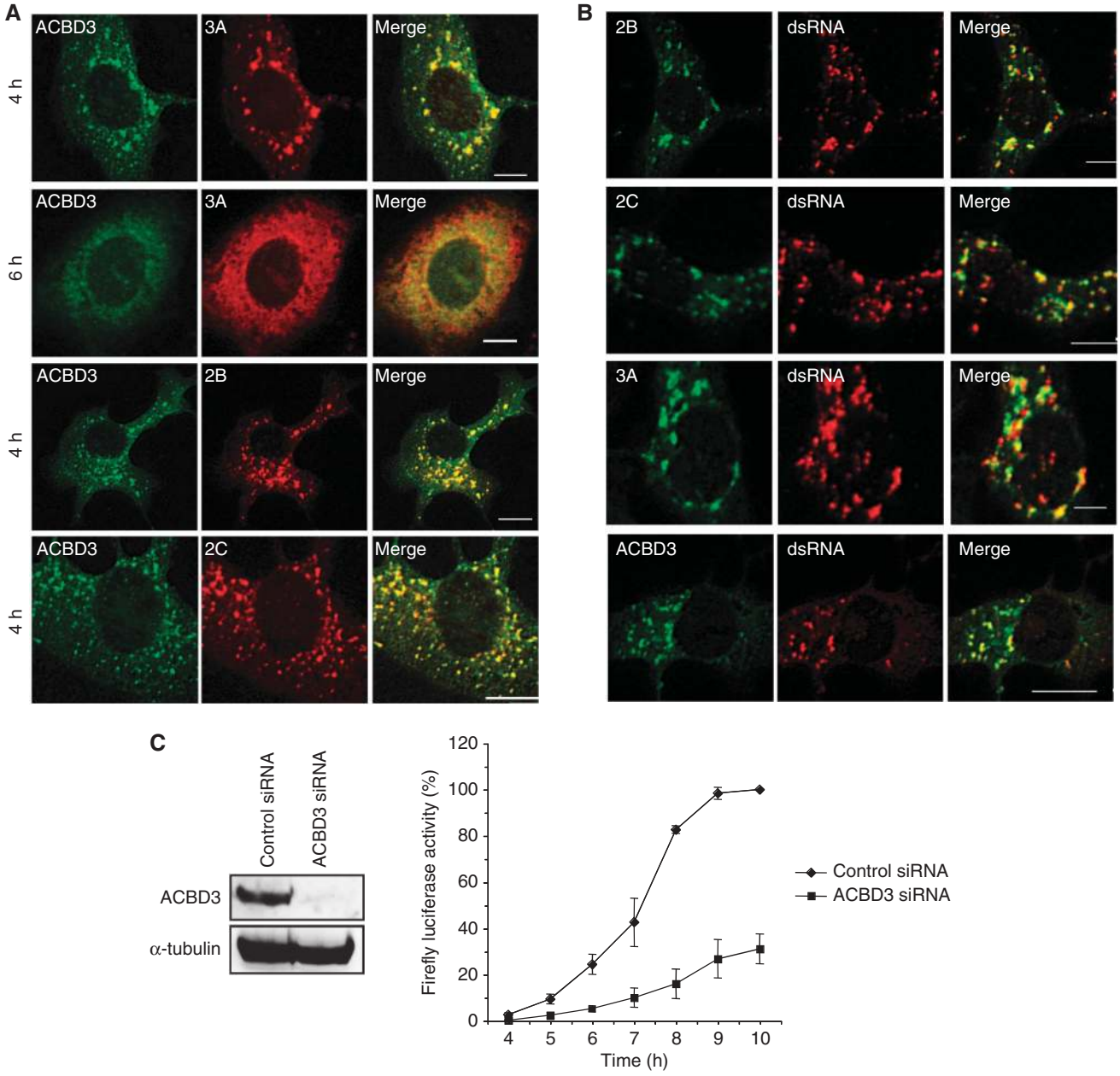

Figure 3 (**A**) Colocalization of ACBD3 with 2B, 2C, and 3A. Vero cells were electroporated with replicon RNA, AV-FL-Luc-5′rzm. At 4 or 6 h after electroporation, the cells were fixed and double stained with rabbit anti-ACBD3 and guinea pig anti-3A, anti-2B, or anti-2C antibodies. (**B**) Colocalization of dsRNA with ACBD3, 2B, 2C, or 3A. Vero cells were electroporated with replicon RNA. At 4 h, the cells were fixed and double stained with anti-dsRNA (mouse) and anti-2B, anti-2C, anti-3A, or anti-ACBD3 antibodies (rabbit). Bars represent 30 μm. (**C**) Effect of knockdown of ACBD3 on AiV replication. Vero cells were transfected with 80 nM of either control siRNA or siRNA against ACBD3. At 72 h after transfection, lysates were prepared and subjected to immunoblotting to assess the levels of ACBD3 and α-tubulin (left panel). At 72 h post transfection with siRNAs, the cells were transfected with replicon RNA and then luciferase activity in cell lysates harvested at the indicated times was measured (right panel). The maximum value obtained for cells treated with control siRNA was taken as 100%. The experiment was repeated at least three times. Standard deviation bars are shown.

was almost completely inhibited at 5 μM (Figure 5A). Cell viability was not affected by treatment with 5 μM (data not shown). It is noted that at 1 h after electroporation, the level of luciferase activity observed for T-00127-HEV1-treated cells was similar to that for cells treated with DMSO, and was significantly higher than that for mock-transfected cells. At this time point, viral RNA replication does not occur, and the obtained luciferase activity mainly results from translation of input RNA (Sasaki and Taniguchi, 2008). Thus, this result suggests that PI4KB activity is important for AiV RNA replication, but not for translation.

Furthermore, we investigated viral RNA replication in PI4KB knockdown cells. Vero cells were treated with siRNA targeting PI4KB or control siRNA. At 72 h after treatment with siRNA targeting PI4KB, a decrease in the amount of PI4KB was observed (Figure 5B). Cell viability was not affected by treatment with siRNA targeting PI4KB (data not shown). At 72 h after siRNA treatment, AV-FL-Luc-5′rzm RNA was

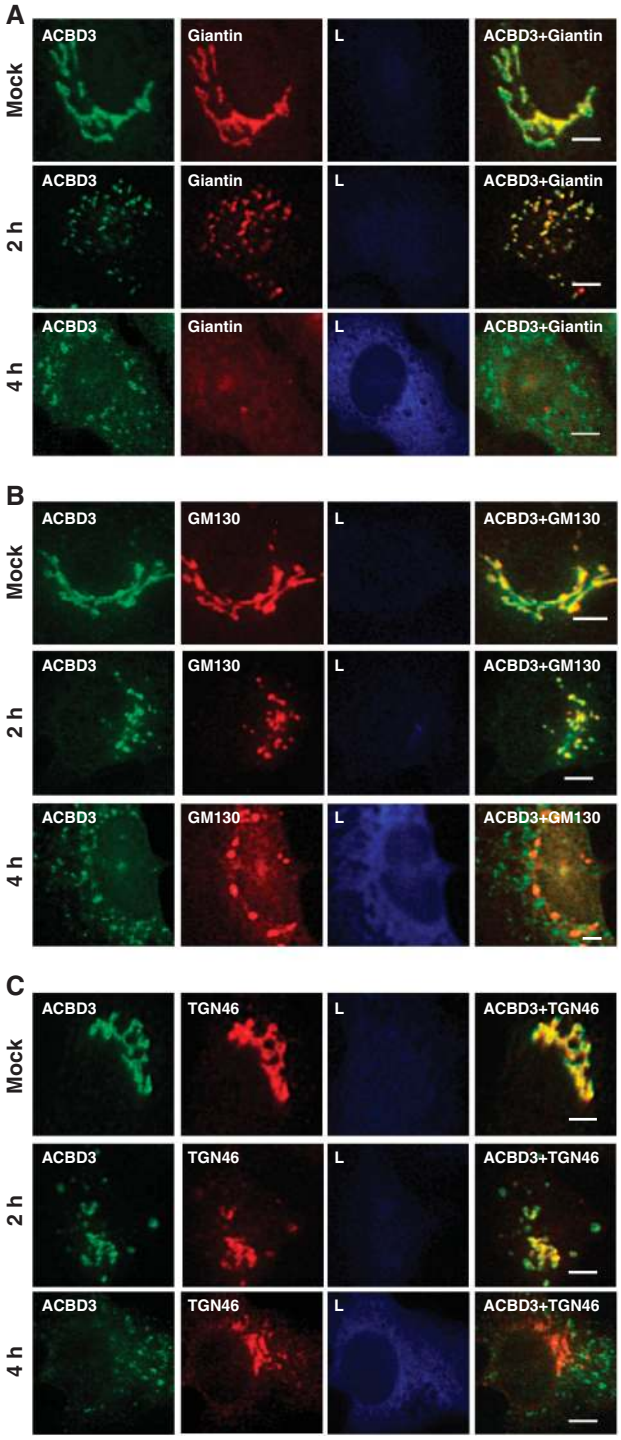

Figure 4 Dynamics of different Golgi proteins during AiV RNA replication. Vero cells were mock electroporated or electroporated with the replicon RNA, AV-FL-Luc-5′rzm. At 2 or 4 h after electroporation, the cells were fixed and triple stained with rabbit anti-ACBD3, guinea pig anti-L, and (**A**) mouse anti-giantin, (**B**) mouse anti-GM130, or (**C**) sheep anti-TGN46 antibodies. Bars represent 30 μm.

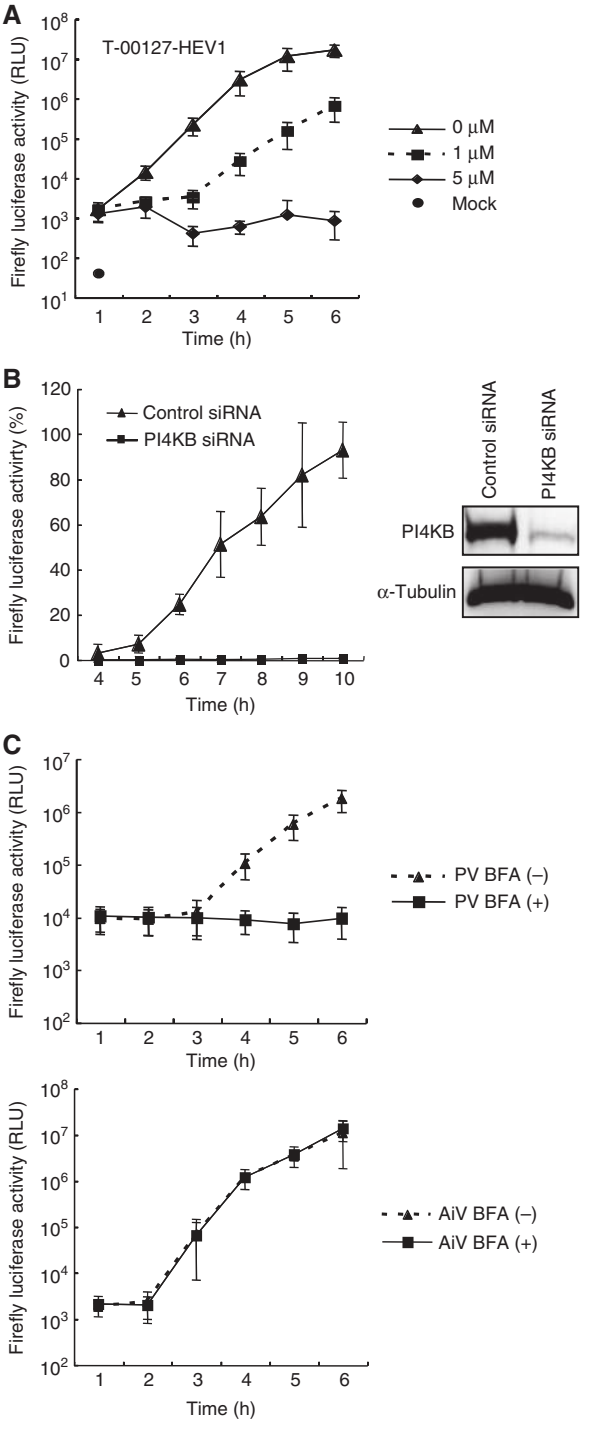

Figure 5 (**A**) T-00127-HEV1 inhibits AiV RNA replication. Vero cells were mock electroporated or electroporated with the replicon RNA, AV-FL-Luc-5′rzm, and then treated with 0 (DMSO), 1 or 5 μM T-00127-HEV1. After incubation for the indicated times, the cells were assayed for luciferase activity. (**B**) Depletion of endogenous PI4KB severely reduces AiV RNA replication. Vero cells were transfected with 40 nM control siRNA or siRNA against PI4KB. At 72 h after transfection, the levels of PI4KB and α-tubulin were determined by immunoblotting (right panel), and the subsequent analysis was performed as in Figure 3C (left panel). (**C**) AiV RNA replication is insensitive to BFA. Vero cells were electroporated with poliovirus (PV) (upper panel) or AiV (lower panel) replicon RNA and then incubated with or without 10 μg/ml of BFA. After incubation for the indicated times, the cells were assayed for luciferase activity. All experiments were repeated at least three times. Standard deviation bars are shown.

transfected by lipofection, and RNA replication was examined by a luciferase assay. Knockdown of PI4KB almost completely inhibited AiV RNA replication, and at 10 h after transfection, luciferase activity was decreased by 99% (Figure 5B). A similar result was obtained using HeLa cells (data not

shown). These results indicate that PI4KB activity is essential for AiV RNA replication.

PI4KB interacts with ACBD3

BFA is an inhibitor of enterovirus RNA replication (Irurzun *et al*, 1992; Maynell *et al*, 1992). BFA inactivates GBF1 (Peyroche *et al*, 1999) and inhibits recruitment of GBF1/Arf1 to 3A, resulting in inhibition of recruitment of PI4KB to the replication sites of enteroviruses (Belov *et al*, 2008; Hsu *et al*, 2010). We investigated whether BFA inhibits AiV replication. Treatment with 10 μg/ml of BFA inhibited poliovirus RNA replication, as known, but did not affect AiV RNA replication at all (Figure 5C). This result suggests that PI4KB is recruited independently of GBF1/Arf1 to the AiV replication sites. As described above, ACBD3 was localized to the Aichi viral RNA replication sites through binding to some viral non-structural proteins. We examined whether ACBD3 interacts with PI4KB. In the mammalian two-hybrid assay, interaction between ACBD3 and PI4KB resulted in a 138-fold increase in luciferase activity, indicating a strong interaction between the two proteins (Figure 6A). No apparent activation of luciferase expression was detected for viral non-structural proteins (3.5-fold increase for 3A and less for other proteins). To further confirm the interaction between ACBD3 and PI4KB, HA-tagged PI4KB was co-expressed with FLAG-tagged ACBD3 or FLAG-tagged 3A in 293T cells, and then co-immunoprecipitation analysis was performed. As shown in Figure 6B, PI4KB was co-immunoprecipitated with ACBD3, but not with 3A, confirming the interaction between ACBD3 and PI4KB.

PI4KB interacts with the central part of ACBD3

To determine the PI4KB-binding domain of ACBD3, interactions of deletion mutants of ACBD3 with PI4KB were investigated in the mammalian two-hybrid system (Figure 6C). Of the five mutants shown in Figure 2A, mut2 and mut5 activated luciferase expression strongly (~15- and 45-fold, respectively), implying the importance of a wider region including aa 171–327 of ACBD3 for binding to PI4KB. Additional two mutants, mut6 and mut7, which contain aa 116–327 and aa 116–428, respectively, exhibited the ability to strongly activate luciferase expression (24- and 32-fold, respectively). These results suggest that the central part of ACBD3 (aa 116–327) is important for binding to PI4KB. In addition, the PI4KB-binding domain was suggested not to overlap with the binding domain for 2B, 2BC, 2C, 3A, and 3AB (aa 374–528).

PI4KB colocalizes with ACBD3, 2B, 2C, 3A, and dsRNA in AiV RNA-transfected cells

We examined whether PI4KB localizes to the viral RNA replication sites. In mock-transfected cells, PI4KB mainly localized to the Golgi, and colocalized with ACBD3 (Figure 7A). When ACBD3 expression was knockdown by using siRNA, PI4KB was dispersed in the cytoplasm and did not localize to the Golgi (Figure 7B), strongly suggesting a critical role of ACBD3 in Golgi recruitment of PI4KB. In viral RNA-replicating cells, PI4KB colocalized with ACBD3, 2B, 2C, 3A, and dsRNA (Figure 7A and C). Treatment of mock-transfected cells with BFA resulted in dispersion of ACBD3 and PI4KB to the cytoplasm (Figure 7D). In contrast, in viral RNA-transfected cells with BFA treatment, ACBD3 and PI4KB

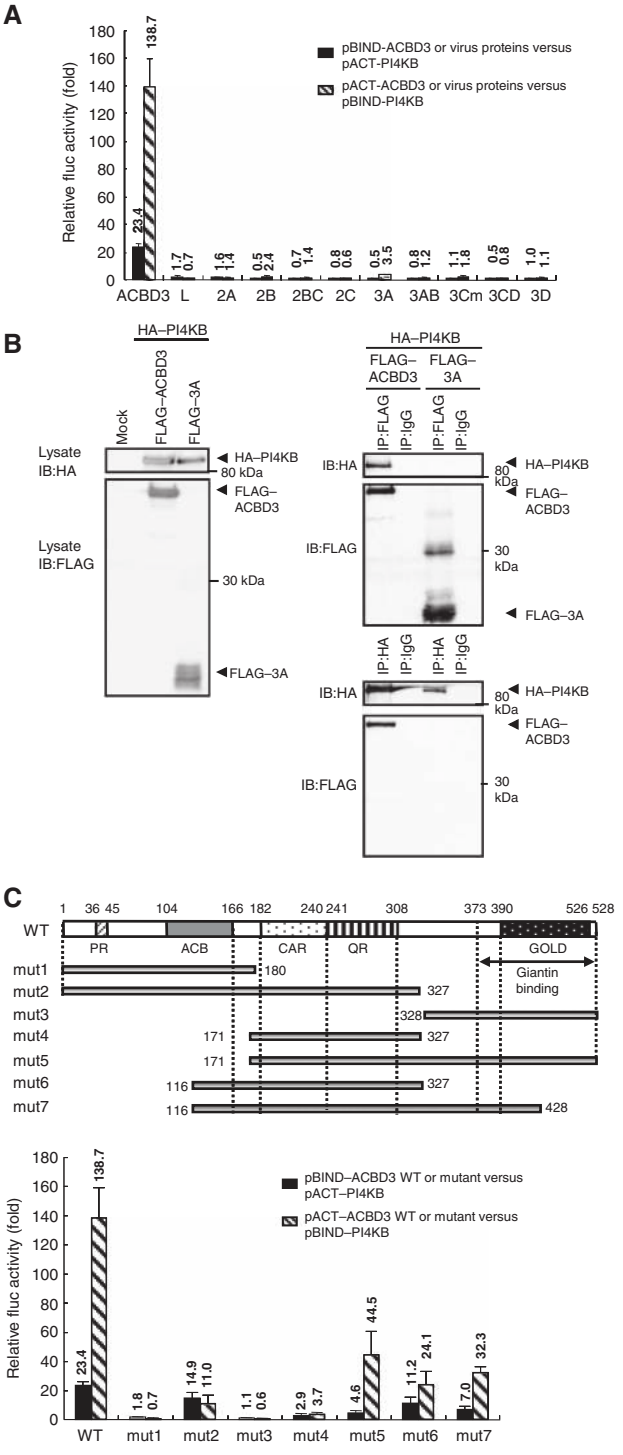

Figure 6 PI4KB interacts with ACBD3. (**A**) The mammalian two-hybrid assay was performed to examine interactions between PI4KB and ACBD3 or the virus proteins and the results are represented as in Figure 1A. (**B**) Co-immunoprecipitation of PI4KB with ACBD3. HA-tagged PI4KB was co-expressed with FLAG-tagged ACBD3 or FLAG-tagged 3A in 293T cells, and the subsequent analysis was performed as in Figure 1B. (**C**) Mapping of the PI4KB-binding region of ACBD3. Schematic representation of full-length ACBD3 (WT) and its mutants (mut6 and mut7) (upper panel). Mammalian two-hybrid analysis was performed to examine interactions between PI4KB and ACBD3 WT or its mutants (mut1–7), and the results are represented as described in Figure 1A (lower panel). Figure source data can be found in Supplementary data.

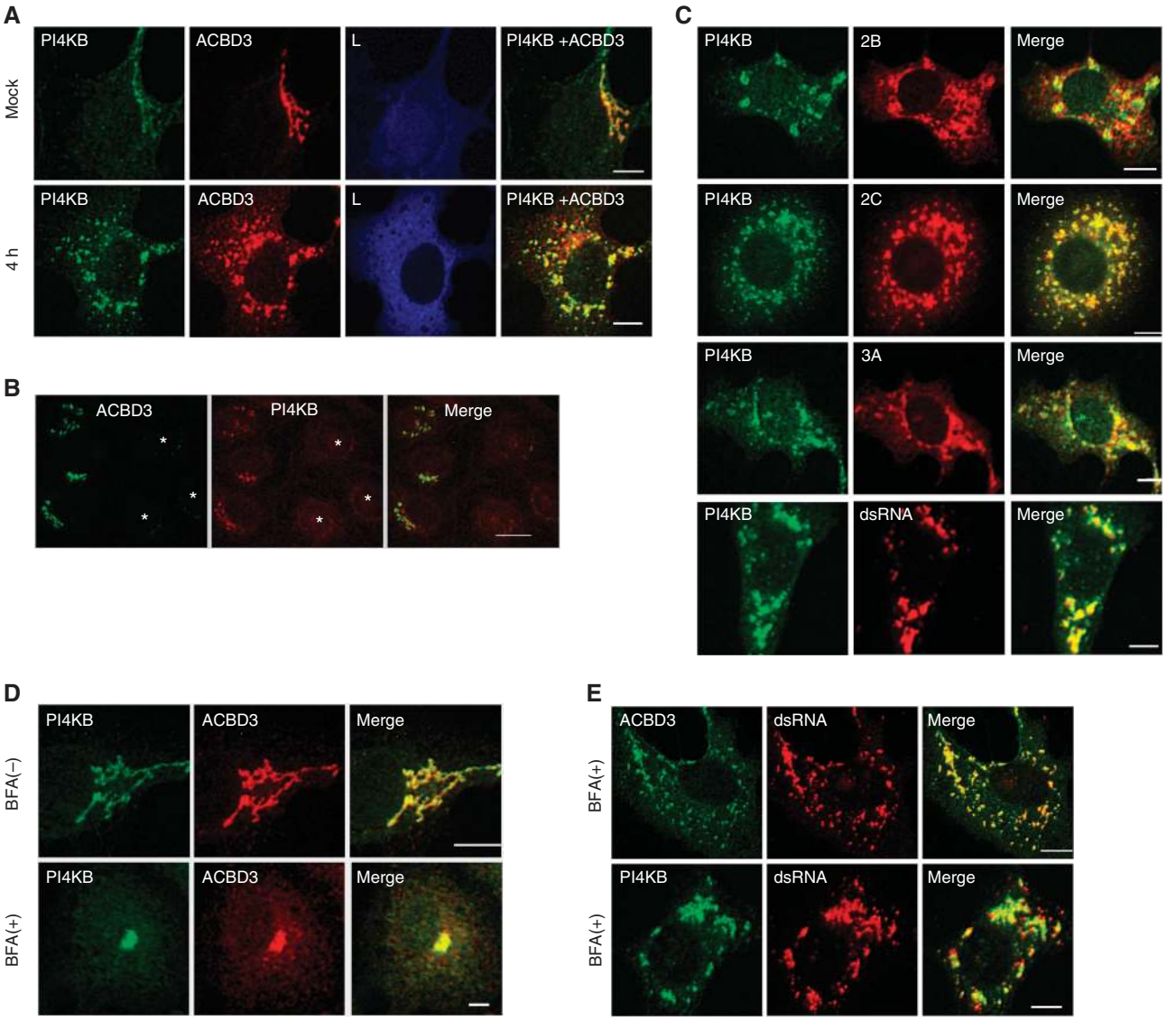

Figure 7 PI4KB is recruited to the AiV RNA replication sites through interaction with ACBD3 associated with the viral proteins. (**A**) Colocalization of PI4KB with ACBD3. Vero cells were mock electroporated or electroporated with the replicon RNA, AV-FL-Luc-5′rzm. At 4 h after electroporation, the cells were fixed and triple stained with mouse anti-PI4KB, rabbit anti-ACBD3, and guinea pig anti-L antibodies. (**B**) Effect of ACBD3 knockdown on the localization of PI4KB. Vero cells were transfected with siRNA against ACBD3. At 72 h after transfection, cells were fixed and double stained with anti-ACBD3 and anti-PI4KB. Asterisks indicate cells where knockdown of the expression of ACBD3 was observed. (**C**) PI4KB colocalizes with 2B, 2C, 3A, or dsRNA. At 4 h after electroporation with the replicon RNA, the Vero cells were fixed and double stained with mouse anti-PI4KB and rabbit anti-2B, -2C, or -3A antibodies, or rabbit anti-PI4KB and mouse anti-dsRNA antibodies. (**D**, **E**) Recruitment of PI4KB and ACBD3 to the AiV RNA replication sites is not affected by BFA. Vero cells were (**D**) mock electroporated or (**E**) electroporated with the replicon RNA, and then incubated in medium with or without 10 μg/ml of BFA. At 4 h after electroporation, the cells were fixed and immunostained with the indicated antibodies. Bars represent 30 μm.

formed clusters in the cytoplasm, and colocalized with dsRNA (Figure 7E). These results indicate that PI4KB is present in the viral RNA replication sites through interaction with ACBD3, which is recruited through interaction with 2B, 2BC, 2C, 3A, and 3AB. In addition, it was shown that recruitment of PI4KB and ACBD3 to the AiV RNA replication sites was not affected by BFA.

PI4P accumulates in viral RNA replication sites

We examined whether recruitment of PI4KB to the sites for AiV RNA replication results in accumulation of PI4P. In mock-transfected cells, PI4P mainly localized to the Golgi, and colocalized with ACBD3 and PI4KB (Figure 8A). In viral RNA-replicating cells, PI4P formed clusters in the cytoplasm, and colocalized with ACBD3, PI4KB, 2B, 2C, 3A, and dsRNA (Figure 8A and B). These results indicate that PI4P accumulates in AiV RNA replication sites.

Discussion

AiV is a member of the family *Picornaviridae*, and belongs to a different genus from the well-characterized picornaviruses, enteroviruses such as poliovirus and CVB3. In this study, we showed that AiV non-structural proteins and cleavage intermediates, 2B, 2BC, 2C, 3A, and 3AB, interact with ACBD3. Furthermore, ACBD3 was shown to interact with PI4KB.

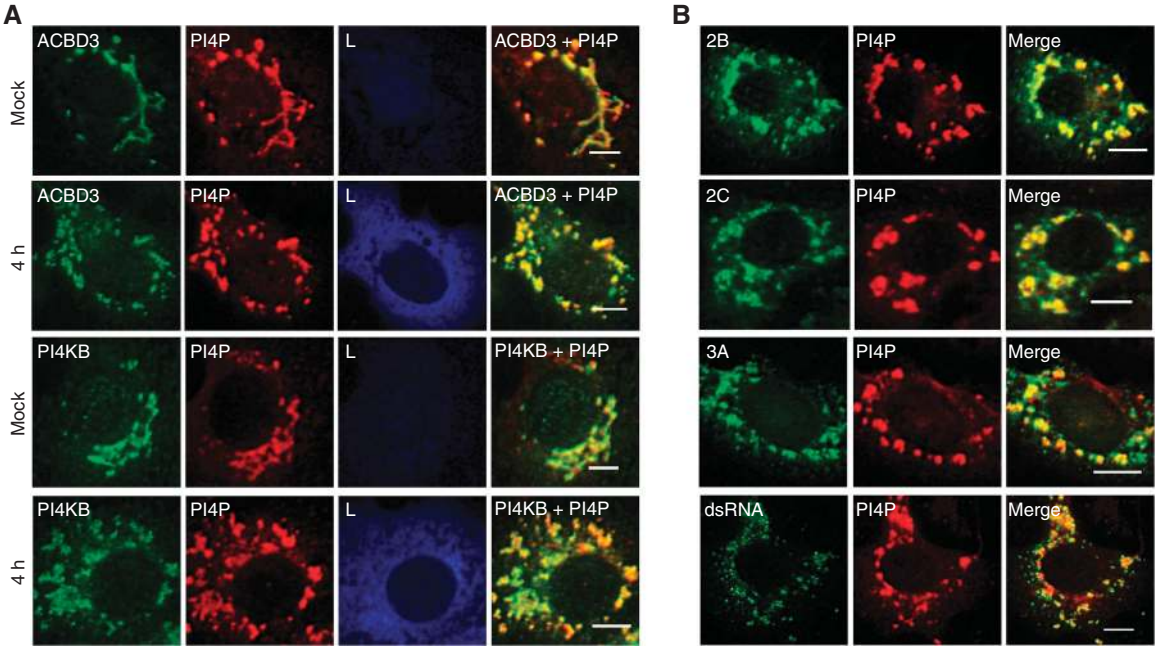

Figure 8 PI4P localizes to the AiV RNA replication sites. (**A**, **B**) Vero cells were electroporated with mock or replicon RNA. At 4 h after electroporation, the cells were fixed and immunostained with the indicated antibodies. Bars represent 30 μm.

Immunofluorescence microscopy showed that dsRNA, which indicates the viral RNA replication sites, colocalized with these viral proteins, ACBD3, PI4KB, and PI4P lipids. In addition, knockdown of ACBD3 or PI4KB using siRNA inhibited AiV RNA replication. These results indicate that the viral protein/ACBD3/PI4KB complex is formed to synthesize PI4P at the viral RNA replication sites and plays an essential role in viral RNA replication.

PI4KB has been reported to be an essential host factor for enterovirus RNA replication (Hsu *et al*, 2010; Arita *et al*, 2011). According to the model proposed by Hsu *et al* (2010), PI4KB is recruited to the RNA replication sites by GBF1/Arf1/3A, and synthesizes PI4P. PI4P can interact with viral RNA polymerase 3D, a soluble protein. Thus, soluble 3D is recruited to the viral RNA replication complex formed on membranes to facilitate viral RNA synthesis. BFA inactivates GBF1 and inhibits the recruitment of GBF1/Arf1 to 3A, thereby inhibiting recruitment of PI4KB to the replication sites of enteroviruses (Belov *et al*, 2008; Hsu *et al*, 2010). The present study showed that AiV replication was insensitive to BFA (Figure 5C). The difference in the sensitivity to BFA between AiV and enteroviruses can be explained by the difference in the strategy used to recruit PI4KB to the viral RNA replication sites. In AiV, PI4KB would be recruited to the viral RNA replication sites through the formation of the viral protein/ACBD3/PI4KB complex. Formation of this complex would be resistant to BFA, as indicated by the observation that PI4KB as well as ACBD3 colocalized with dsRNA even in the presence of BFA (Figure 7E). This result is in contrast to the observation that PI4KB disperses in BFA-treated CVB3-infected cells (Hsu *et al*, 2010). It remains to be determined whether PI4P can bind to AiV 3D RNA polymerase.

It is known that PI4KB is recruited to the Golgi by Arf1 (Godi *et al*, 1999). The present study would be the first report that PI4KB interacts with ACBD3. Knockdown of ACBD3 resulted in abrogation of Golgi localization of PI4KB (Figure 7B), suggesting a critical role of ACBD3 in Golgi recruitment of PI4KB. ACBD3 is also known as peripheral-type benzodiazepine receptor and cAMP-dependent protein kinase-associated protein 7 (PAP7) (Li *et al*, 2001) or Golgi complex-associated protein of 60 kDa (GCP60) (Sohda *et al*, 2001). ACBD3 is localized to the Golgi and also to mitochondria (Li *et al*, 2001; Sohda *et al*, 2001), and has various biological functions (reviewed in Fan *et al*, 2010) in the maintenance of the Golgi apparatus structure (Sohda *et al*, 2001), apoptosis (Sbodio *et al*, 2006), steroidogenesis (Li *et al*, 2001), neurogenesis (Cheah *et al*, 2006), and embryogenesis (Zhou *et al*, 2007). Studies to elucidate the biological significance of the interaction between ACBD3 and PI4KB will help to further understand the biological functions of these proteins.

ACBD3 contains no hydrophobic region that can be involved in membrane localization, and is localized to the Golgi through interaction with giantin, which contains a C-terminal membrane-anchoring domain (Sohda *et al*, 1994, 2001). The giantin-binding domain of ACBD3 has been mapped to the C-terminal region (aa 373–528). Our mammalian two-hybrid assays indicated that the giantin-binding domain of ACBD3 overlapped with the binding domain for the five viral nonstructural proteins (aa 374–528) (Figure 2), but did not overlap with the PI4KB-binding domain, which was mapped to the central region (aa 116–327) (Figure 6C). This implies that PI4KB is at least partly present in the Golgi through interaction with the ACBD3/giantin complex. We propose a model for recruitment of PI4KB to the AiV RNA replication sites (Figure 9). The viral membrane proteins 2B, 2BC, 2C, 3A, and 3AB will compete with giantin for binding to ACBD3 at the Golgi. As infection progresses, the viral proteins will rob the preexisting giantin/ACBD3/PI4KB complex of the ACBD3/PI4KB complex to form the viral protein/ACBD3/PI4KB complex. This is also suggested by the subcellular localization of these proteins shown in Figures 3, 4A, and 7.

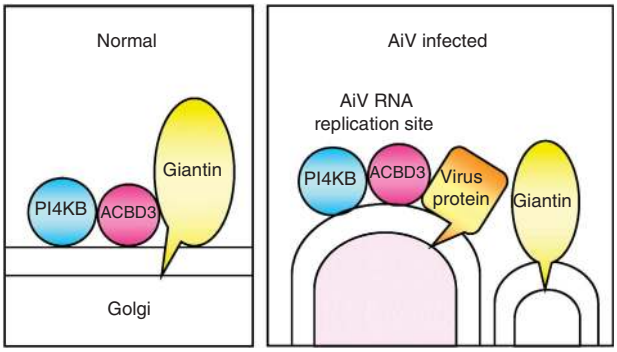

Figure 9 Model for recruitment of PI4KB to the AiV replication sites. In uninfected cells, the C-terminal region of ACBD3 binds to the C-terminal cytoplasmic domain of giantin that is anchored to the Golgi membrane through the C-terminal anchoring domain. PI4KB is localized to the Golgi through interaction with the central part of ACBD3 (left panel). In AiV-infected cells, viral membrane proteins 2B, 2BC, 2C, 3A, and 3AB compete with giantin at the Golgi for binding to ACBD3. The viral protein/ACBD3/PI4KB complex is formed as infection progresses, whereas giantin no longer colocalizes with ACBD3 (right panel).

ACBD3 targeting of the multiple viral proteins may result in increases in the concentrations of the viral proteins at the Golgi to facilitate formation of viral replication complexes. In addition, binding of multiple viral proteins to ACBD3 that has the ability to associate with PI4KB would lead to efficient recruitment of PI4KB to the viral RNA replication sites.

The redistribution of giantin, GM130, and TGN46 to the cytoplasm observed in AiV-replicating cells (Figure 4) indicates Golgi disassembly. It has been reported that ACBD3 is involved in the maintenance of the Golgi structure by interacting with giantin (Sohda *et al*, 2001). Dissociation of ACBD3 from giantin through bound by the viral proteins may contribute to Golgi disassembly. At 4 h after electroporation with the replicon RNA, 2B, 2C, and 3A colocalized with ACBD3 in patchy structures in the cytoplasm (Figure 3A). On the other hand, giantin, GM130, and TGN46 redistributed to the cytoplasm did not colocalize with ACBD3 (Figure 4). Considering that the virus membrane proteins 2B, 2C, and 3A target ACBD3, it is very likely that these viral proteins are first accumulated in the Golgi, and then the replication complexes are formed utilizing Golgi membranes; however, the mechanism of the membrane remodelling for formation of the AiV replication complexes is currently unknown. Interestingly, acyl-coenzyme A (acyl-CoA) has been reported to participate in the budding of transport vesicles from Golgi cisternae and the fusion of transport vesicles with Golgi cisternae (Glick and Rothman, 1987; Pfanner *et al*, 1989, 1990). ACBD3-bound acyl-CoA may play a role in membrane remodelling for formation of the viral RNA replication complexes. In addition, the absence of three Golgi proteins, giantin, GM130, and TGN46, at the AiV RNA replication sites suggests the sorting or deterring of Golgi components, which has been observed in CVB3-infected cells (Hsu *et al*, 2010). TGN46 is present at the sites for CVB3 replication, but was absent at the AiV replication sites. On the other hand, the absence of GM130 was observed in the replication sites for the two viruses. These imply a different manner of sorting or deterring of the Golgi components between AiV and CVB3. Analysis of the subcellular localization of other Golgi components and factors involved in intracellular membrane traffic in AiV-infected cells will be required for elucidation of the mechanism of formation of the AiV replication complexes.

The C-terminal region of ACBD3 interacting with the AiV proteins as well as giantin is known as the GOLD (Golgi dynamics) domain (Figure 2A). The GOLD domain is typically 90–150 aa long and folds into six or seven β-strands. This domain has been identified in several proteins with roles in Golgi dynamics and secretion including p24 proteins and Sec14 proteins, and is thought to serve as a common denominator in protein–protein interactions (Anantharaman and Aravind, 2002). It would be interesting to investigate whether the AiV proteins have the ability to bind to other GOLD domain-containing proteins.

In conclusion, the present study demonstrated that AiV utilized a different strategy to recruit PI4KB to the replication sites from enteroviruses, that is, through viral protein/ACBD3/PI4KB interactions. ACBD3-mediated recruitment of PI4KB to the replication sites was resistant to BFA. The sensitivity of viral replication to BFA varies among different picornaviruses. HAV is sensitive and human parechovirus is partly sensitive. On the other hand, FMDV and encephalomyocarditis virus are insensitive (Blank *et al*, 2000; Gazina *et al*, 2002; Monaghan *et al*, 2004). It would be of interest to investigate whether all picornaviruses require PI4KB for replication and, if so, how PI4KB is recruited to the replication sites.

Materials and methods

Cell lines and reagents

Vero (African green monkey kidney cell line) and 293T (human embryonic kidney cell line) cells were maintained in Eagle's minimum essential medium supplemented with 5 and 10% fetal bovine serum, respectively, at 37°C. BFA was purchased from Sigma, and diluted in ethanol. T-00127-HEV1 was described previously (Arita *et al*, 2011), and diluted in DMSO.

Replicon RNAs of AiV and poliovirus

The AiV and poliovirus replicon RNAs containing a firefly luciferase gene (AV-FL-Luc-5′rzm RNA and PV-Fluc mc RNA, respectively) were generated by *in-vitro* transcription using a T7 RiboMAX express large scale RNA production system (Promega) from *Hin*dIII-linearized pAV-FL-Luc-5′rzm (Sasaki and Taniguchi, 2003; Nagashima *et al*, 2005) and *Dra*I-linearized pPV-Fluc mc (Arita *et al*, 2006), respectively. Lysates of cells transfected with the replicon RNAs were prepared using a Passive lysis buffer (Promega) and subjected to a luciferase assay using a Luciferase assay system (Promega) and a luminometer, Lumat LB9507 (Berthold).

Plasmids

The construction of pBIND-L, -2A, -2B, -2BC, -2C, -3A, -3AB, -3Cm, -3CD, and -3D, and pACT-L, -2A, -2B, -2BC, -2C, -3A, -3AB, -3Cm, -3CD, and -3D was described previously (Ishikawa *et al*, 2010). The coding region of ACBD3 was amplified by PCR from a cDNA clone (Toyobo, FCC137B01), while the PI4KB-coding sequence was amplified by RT–PCR using total RNA prepared from HeLa cells. Each PCR product was cloned into pBIND and pACT (Promega) as described previously (Ishikawa *et al*, 2010), yielding pBIND-ACBD3 and -PI4KB, and pACT-ACBD3 and -PI4KB. pBIND and pACT constructs encoding ACBD3 deletion mutants (pBIND- or pACT-ACBD3-mut1, -mut2, -mut3, -mut4, -mut5, -mut6, -mut7, -mut3Δ1, -mut3Δ2, -mut3Δ3, -mut3Δ4, and -mut3Δ5) were generated by cloning each DNA fragment amplified by PCR from pACT-ACBD3 into pBIND and pACT. The DNA fragments encoding L, 2B, 2BC, 2C, 3A, and 3AB were obtained by PCR from pAV-FL-Luc-5′rzm. The PCR-amplified DNA fragment encoding L, 2B, 2BC, 2C, 3A, 3AB, PI4KB, or ACBD3 was cloned into pCI mammalian expression vector (Promega) containing an HA or FLAG tag-coding sequence to

produce an N-terminally HA- or FLAG-tagged protein (pCI-HA–L, pCI-HA–2B, pCI-HA–2BC, pCI-HA–2C, pCI-HA–3A, pCI-HA–3AB, and pCI-HA–PI4KB, and pCI-FLAG–3A and pCI-FLAG–ACBD3). To construct bait plasmids for the yeast two-hybrid assays, the 2B-, 2C- and 3A-coding regions were amplified by PCR and then cloned into pGBKT7 (Clontech), resulting in pGBKT7-2B, -2C, and -3A. The nucleotide sequences of all the PCR products were verified. For expressing MBP-fused 2B, 2C, or 3A in *E. coli*, these genes were amplified by PCR and cloned into pMAL-c2X (New England Biolabs). pMAL-3AB was described previously (Nagashima *et al*, 2008). For expressing GST-fused ACBD3, PCR-amplified ACBD3-coding sequence was cloned into pGEX-6P3 (Amersham Pharmacia Biotech).

Antibodies

Rabbit or guinea pig polyclonal antibody to 3A was obtained by immunization with the His-tagged 3A protein expressed in *Escherichia coli*. Rabbit or guinea pig polyclonal antibodies to 2B and 2C were obtained by immunization with a mixture of two peptides (2B: GLLTLSADTETNQTLNKC and SQFDLSGPANSV-SLAASC; and 2C: CPFDPTNALNPIPGTQSK and IRGKAKTDPQAK-LADVHC). The preparation of guinea pig polyclonal antibody to L was described previously (Sasaki *et al*, 2003). Mouse monoclonal antibodies to HA tag, FLAG tag, ACBD3 (clone G2G), and α-tubulin, and rabbit polyclonal antibodies to FLAG tag and ACBD3 were purchased from Sigma; mouse monoclonal antibody to GST from Wako; rabbit polyclonal antibody to HA tag from Bethyl; rabbit polyclonal antibody to PI4KB from Millipore; mouse monoclonal antibodies to GM130 and PI4KB from BD Biosciences; mouse monoclonal antibody to giantin from Abcam; sheep polyclonal antibody to TGN46 was from AbD serotec; anti-PI4P antibody (mouse monoclonal IgM) from Echelon Biosciences; mouse monoclonal antibody to dsRNA (clone J2) from English and Scientific Consulting; Alexa Fluor 488-conjugated anti-mouse IgG and anti-rabbit IgG antibodies, Alexa Fluor 594-conjugated anti-mouse IgG, anti-mouse IgM, anti-rabbit IgG, anti-sheep IgG, and anti-guinea pig IgG antibodies from Molecular Probes; AMCA-conjugated anti-guinea pig IgG from Millipore; and horseradish peroxidase (HRP)-conjugated antibodies from Zymed.

Yeast two-hybrid assays

Yeast two-hybrid assays were performed with a Matchmaker two-hybrid system 3 (Clontech) according to the manufacturer's instructions. The bait plasmid encoding 2B, 2C or 3A, pGBKT-2B, -2C or -3A, was transformed into *Saccharomyces cerevisiae* strain AH109, and the individual transformants were mated with *S. cerevisiae* strain Y187 pretransformed with a human HeLa cDNA library (Clontech) constructed in pGADT7. The resulting diploids were screened on agar plates of dropout medium lacking adenine, histidine, leucine, and tryptophan, supplemented with X-alpha-Gal (5-bromo-4-chloro-3-indolyl-alpha-*O*-galactopyranoside). The insert DNAs of yeast clones grown on plates were amplified by PCR and sequenced directly.

Mammalian two-hybrid assays

The mammalian two-hybrid assays were performed as described previously using a Checkmate mammalian two-hybrid system (Promega) (Ishikawa *et al*, 2010). The ability of viral protein gene-containing constructs to express fusion proteins was examined previously (Ishikawa *et al*, 2010). Expression of the ACBD3 constructs and deletion mutants were also examined by immunoblotting as described previously (Ishikawa *et al*, 2010) and confirmed expression of fusion proteins for mutants that exhibited no increase in luciferase activity (data not shown).

DNA transfection, immunoprecipitation, and immunoblotting

Transfection of plasmid DNA was carried out using a FuGENE HD transfection reagent (Roche) according to the manufacturer's protocol. For the immunoprecipitation assays, 293T cells were grown in 6-well plates for 24 h and then transfected with HA- and FLAG-tagged constructs (2 μg/well). At 24 h (for co-expression of HA–2B, HA–2C, HA–3A, or HA–PI4KB) or 48 h (for co-expression of HA–2BC or HA–3AB) after transfection, cells were washed three times with phosphate-buffered saline (PBS) and then lysed in 350 μl lysis buffer (50 mM Tris–HCl, pH 8.0, 150 mM NaCl, 1% or 0.2% Nonidet P-40 (NP-40), 1 mM phenylmethylsulphonyl fluoride) supplemented with a protease inhibitor cocktail and a phosphatase inhibitor cocktail (Sigma). Cell lysates were centrifuged at 12 000 *g* for 10 min, and the supernatants were immunoprecipitated with 50 μl of Dynabeads Protein G (Dynal) coated with 1 μg of antibody at 4°C for 1 h. After washing three times with lysis buffer and then one time with wash buffer (50 mM Tris–HCl pH 8.0), the beads were boiled in SDS–PAGE sample buffer. The immunoprecipitates were separated by 12.5% or 7.5% SDS–PAGE and then transferred onto polyvinylidene difluoride membranes (Bio-Rad). The membranes were probed with appropriate primary antibodies, followed by incubation with HRP-conjugated secondary antibodies. The chemiluminescence signals were visualized using ECL Advance reagents (Amersham Biosciences) and an LAS-4000UVmini (Fujifilm).

MBP pull-down assay

MBP, MBP–2B, MBP–2C, MBP–3A, and MBP–3AB, and GST–ACBD3 were expressed in *E. coli* BL21 cells according to the manufacturer's protocols. For purifying GST–ACBD3, harvested cells were suspended in Buffer A (140 mM NaCl, 2.7 mM KCl, 10 mM Na_2HPO_4, 1.8 mM KH_2PO_4, pH 7.4) and lysed by sonication. The lysate was mixed with 50% glutathione-Sepharose slurry (GE Healthcare) and incubated for 4 h at 4°C. After the beads were washed three times with Buffer A, GST–ACBD3 were eluted with elution buffer (50 mM Tris–HCl, 10 mM reduced glutathione, pH 8.0). Cells expressing MBP or MBP-fused viral proteins were suspended in Column buffer (20 mM Tris–HCl, 200 mM NaCl, 1 mM EDTA, pH 7.5) and lysed by sonication, and the lysates were incubated with 7.5 μl of 50% amylose resin slurry (New England Biolabs) for 90 min at 4°C. Then, the resin was washed three times with Column buffer, resuspended in NP-40 buffer (50 mM Tris–HCl, 150 mM NaCl, 1% NP-40, pH 8.0), and then mixed with purified GST–ACBD3. After incubation for 90 min at 4°C, the resin was washed five times with NP-40 buffer. Proteins binding to the resin were eluted with Column buffer containing 10 mM maltose, and analysed by SDS–PAGE, followed by immunoblotting with anti-GST antibody and Coomassie brilliant blue (CBB) staining.

Electroporation and immunofluorescence microscopy

Electroporation was performed as described previously (Sasaki *et al*, 2001). Vero cells mock electroporated or electroporated with replicon RNA were cultured on slide glasses. For BFA treatment, the electroporated cells were cultured in medium containing 10 μg/ml of BFA for 4 h. At appropriate times after electroporation, the cells were fixed with PBS containing 4% paraformaldehyde for 45 min and then permeabilized with PBS containing 0.5% Triton X-100 for 15 min or PBS containing 20 μM digitonin for 5 min only for staining PI4P. The cells were incubated with appropriate primary antibodies and then with appropriate secondary antibodies diluted in PBS containing 3% bovine serum albumin or can get signal immunostain solution A (Toyobo). The slide glasses were mounted with Fluoromount Plus (Diagnostic BioSystems) and then viewed under a fluorescence microscope, BZ-8000 (Keyence).

Gene silencing with siRNA

Control siRNA (ON-TARGET plus non-targeting siRNA#1), and siRNAs against ACBD3 and PI4KB (ON-TARGET plus SMART pool siRNA) were purchased from Dharmacon. The target sequences for ACBD3 and PI4KB were as follows: 5′-GGAUGCAGAUUCCGUGAUU-3′ (ACBD3 siRNA1), 5′-GCAACUGUACCAAGUAAUA-3′ (ACBD3 siRNA2), 5′-GCAUAUGGGAAGUAACAUU-3′ (ACBD3 siRNA3), 5′-GUAUAGAAACCAUGGAGUU-3′ (ACBD3 siRNA4), 5′-CCUUUAAGC UGACCACAGA-3′ (PI4KB siRNA1), 5′-CCGAGAGUAUUGAUAAUUC-3′ (PI4KB siRNA2), 5′-CCCAGUUGCUUAACAUGUA-3′ (PI4KB siRNA3), and 5′-GGACUCACCAGCGCUCUAA-3′ (PI4KB siRNA4). A mixture of these four siRNAs was used for gene silencing of ACBD3 or PI4KB. Vero cells grown on a 48-well plate were transfected with 40 or 80 nM of siRNA using Lipofectamine RNAiMAX (Invitrogen) according to the manufacturer's protocol. The transfected cells were grown for 72 h and subjected to the following analyses. The levels of ACBD3 and PI4KB expression were evaluated by immunoblotting. Cell viability was measured using a Calcein AM Cell Viability Kit (Trevigen) according to the manufacture's protocol and calcein fluorescence was detected using a 2030 ARVO X multilabel plate reader (Perkin-Elmer). Transfection of siRNA-treated cells with the replicon RNA for the luciferase assay was performed by using Lipofectin reagent (Invitrogen) as described previously (Sasaki *et al*, 2001).

Acknowledgements

This study was supported in part by Grant-in-Aid for Scientific Research (C), and Grant-in-Aid for Scientific Research on Priority Areas: Matrix of Infection Phenomena from the Ministry of Education, Culture, Sports, Science and Technology, and Grant-in-Aid from the Ministry of Health, Labor and Welfare, Japan.

Author contributions: JS designed the experiments, performed experiments shown in Figure 1C, 5A and C, and wrote the manuscript. KI performed most of the experiments, analysed the results, and wrote the manuscript. MA contributed with important reagents and discussed the data. KT coordinated the study and oversaw the research.

Conflict of interest

The authors declare that they have no conflict of interest.

References

Aldabe R, Barco A, Carrasco L (1996) Membrane permeabilization by poliovirus proteins 2B and 2BC. *J Biol Chem* **271:** 23134–23137

Ambert-Balay K, Lorro M, Bon F, Giraudon H, Kaplon J, Wolfer M, Lebon P, Gendrel D, Pothier P (2008) Prevalence and genetic diversity of Aichi virus in community and hospitalized patients. *J Clin Microbiol* **46:** 1252–1258

Anantharaman V, Aravind L (2002) The GOLD domain, a novel protein module involved in Golgi function and secretion. *Genome Biol* **3:** research0023

Arita M, Kojima H, Nagano T, Okabe T, Wakita T, Shimizu H (2011) Phosphatidylinositol 4-kinase III beta is a target of enviroxime-like compounds for antipoliovirus activity. *J Virol* **85:** 2364–2372

Arita M, Nagata N, Sata T, Miyamura T, Shimizu H (2006) Quantitative analysis of poliomyelitis-like paralysis in mice induced by a poliovirus replicon. *J Gen Virol* **87:** 3317–3327

Belov GA, Altan-Bonnet N, Kovtunovych G, Jackson CL, Lippincott-Schwartz J, Ehrenfeld E (2007) Hijacking components of the cellular secretory pathway for replication of poliovirus RNA. *J Virol* **81:** 558–567

Belov GA, Feng Q, Nikovics K, Jackson CL, Ehrenfeld E (2008) A critical role of a cellular membrane traffic protein in poliovirus RNA replication. *PLoS Pathog* **4:** e1000216

Belov GA, Fogg MH, Ehrenfeld E (2005) Poliovirus proteins induce membrane association of GTPase ADP-ribosylation factor. *J Virol* **79:** 7207–7721

Berger KL, Cooper JD, Heaton NS, Yoon R, Oakland TE, Jordan TX, Mateu G, Grakoui A, Randall G (2009) Roles for endocytic trafficking and phosphatidylinositol 4-kinase III alpha in hepatitis C virus replication. *Proc Natl Acad Sci USA* **106:** 7577–7582

Blank CA, Anderson DA, Beard M, Lemon SM (2000) Infection of polarized cultures of human intestinal epithelial cells with hepatitis A virus: vectorial release of progeny virions through apical cellular membranes. *J Virol* **74:** 6476–6484

Cheah JH, Kim SF, Hester LD, Clancy KW, Patterson III SE, Papadopoulos V, Snyder SH (2006) NMDA receptor-nitric oxide transmission mediates neuronal iron homeostasis via the GTPase Dexras1. *Neuron* **51:** 431–440

Cho MW, Teterina N, Egger D, Bienz K, Ehrenfeld E (1994) Membrane rearrangement and vesicle induction by recombinant poliovirus 2C and 2BC in human cells. *Virology* **202:** 129–145

DeWitte-Orr SJ, Mehta DR, Collins SE, Suthar MS, Gale Jr M, Mossman KL (2009) Long double-stranded RNA induces an antiviral response independent of IFN regulatory factor 3, IFN-β promoter stimulator 1, and IFN. *J Immunol* **183:** 6545–6553

Egger D, Teterina N, Ehrenfeld E, Bienz K (2000) Formation of the poliovirus replication complex requires coupled viral translation, vesicle production, and viral RNA synthesis. *J Virol* **74:** 6570–6580

Fan J, Liu J, Culty M, Papadopoulos V (2010) Acyl-coenzyme A binding domain containing 3 (ACBD3; PAP7; GCP60): An emerging signaling molecule. *Prog Lipid Res* **49:** 218–234

Gazina EV, Mackenzie JM, Gorrell RJ, Anderson DA (2002) Differential requirements for COPI coats in formation of replication complexes among three genera of *Picornaviridae*. *J Virol* **76:** 11113–11122

Glick BS, Rothman JE (1987) Possible role for fatty acyl-coenzyme A in intracellular protein transport. *Nature* **326:** 309–312

Godi A, Pertile P, Meyers R, Marra P, Di Tullio G, Iurisci C, Luini A, Corda D, De Matteis MA (1999) ARF mediates recruitment of PtdIns-4-OH kinase-β and stimulates synthesis of PtdIns(4,5)P_2 on the Golgi complex. *Nat Cell Biol* **1:** 280–287

Goyer M, Aho LS, Bour JB, Ambert-Balay K, Pothier P (2008) Seroprevalence distribution of Aichi virus among a French population in 2006–2007. *Arch Virol* **153:** 1171–1174

Harwood LJ, Gerber H, Sobrino F, Summerfield A, McCulloug KC (2008) Dendritic cell internalization of foot-and-mouth disease virus: influence of heparan sulfate binding on virus uptake and induction of the immune response. *J Virol* **82:** 6379–6394

Hsu NY, Ilnytska O, Belov G, Santiana M, Chen YH, Takvorian PM, Pau C, van der Schaar H, Kaushik-Basu N, Balla T, Cameron CE, Ehrenfeld E, van Kuppeveld FJM, Altan-Bonnet N (2010) Viral reorganization of the secretory pathway generates distinct organelles for RNA replication. *Cell* **141:** 799–811

Hyde JL, Sosnovtsev SV, Green KY, Wobus C, Virgin HW, Mackenzie JM (2009) Mouse norovirus replication is associated with virus-induced vesicle clusters originating from membranes derived from the secretory pathway. *J Virol* **83:** 9709–9719

Irurzun A, Perez L, Carrasco L (1992) Involvement of membrane traffic in the replication of poliovirus genomes: effects of brefeldin A. *Virology* **191:** 166–175

Ishikawa K, Sasaki J, Taniguchi K (2010) Overall linkage map of the nonstructural proteins of Aichi virus. *Virus Res* **147:** 77–84

Jackson WT, Giddings TH, Taylor MP, Mulinyawe S, Rabinovitch M, Kopito RR, Kirkegaard K. (2005) Subversion of cellular autophagosomal machinery by RNA viruses. *PLoS Biol* **3:** e156

Knoops K, Kikkert M, van den Worm SHE, Zevenhoven-Dobbe JC, van der Meer Y, Koster AJ, Mommaas AM, Snijder EJ (2008) SARS-coronavirus replication is supported by a reticulovesicular network of modified endoplasmic reticulum. *PLoS Biol* **6:** e226

Knox C, Moffat K, Ali S, Ryan M, Wileman T (2005) Foot-and-mouth disease virus replication sites form next to the nucleus and close to the Golgi apparatus, but exclude marker proteins associated with host membrane compartments. *J Gen Virol* **86:** 687–696

Krogerus C, Samuilova O, Pöyry T, Jokitalo E, Hyypiä T (2007) Intracellular localization and effects of individually expressed human parechovirus 1 non-structural proteins. *J Gen Virol* **88:** 831–841

Lanke KHW, van der Schaar HM, Belov GA, Feng Q, Duijsings D, Jackson CL, Ehrenfeld E, van Kuppeveld FJM (2009) GBF1, a guanine nucleotide exchange factor for Arf, is crucial for coxsackievirus B3 RNA replication. *J Virol* **83:** 11940–11949

Li H, Degenhardt B, Tobin D, Yao ZX, Tasken K, Papadopoulos V (2001) Identification, localization, and function in steroidogenesis of PAP7: a peripheral-type benzodiazepine receptor- and PKA (RIalpha)-associated protein. *Mol Endocrinol* **15:** 2211–2228

Maynell LA, Kirkegaard K, Klymkowsky MW (1992) Inhibition of poliovirus RNA synthesis by brefeldin A. *J Virol* **66:** 1985–1994

Miller S, Krijnse-Locker J (2008) Modification of intracellular membrane structures for virus replication. *Nat Rev Microbiol* **6:** 363–374

Miller S, Sparacio S, Bartenschlager R (2006) Subcellular localization and membrane topology of the Dengue virus type 2 nonstructural protein 4B. *J Biol Chem* **281:** 8854–8863

Moffat K, Howell G, Knox C, Belsham GJ, Monaghan P, Ryan MD, Wileman T (2005) Effects of foot-and-mouth disease virus nonstructural proteins on the structure and function of the early secretory pathway: 2BC but not 3A blocks endoplasmic reticulum-to-Golgi transport. *J Virol* **79:** 4382–4395

Monaghan P, Cook H, Jackson T, Ryan M, Wileman T (2004) The ultrastructure of the developing replication site in foot-and-mouth disease virus-infected BHK-38 cells. *J Gen Virol* **85:** 933–946

Nagashima S, Sasaki J, Taniguchi K (2005) The 5′-terminal region of the Aichi virus genome encodes *cis*-acting replication elements required for positive- and negative-strand RNA synthesis. *J Virol* **79:** 6918–6931

Nagashima S, Sasaki J, Taniguchi K (2008) Interaction between polypeptide 3ABC and the 5′-terminal structural elements of the

genome of Aichi virus: implication for negative-strand RNA synthesis. *J Virol* **82:** 6161–6171

Oh DY, Silva PA, Hauroeder B, Diedrich S, Cardoso DDP, Schreier E (2006) Molecular characterization of the first Aichi viruses isolated in Europe and in South America. *Arch Virol* **151:** 1199–1206

Peyroche A, Antonny B, Robineau S, Acker J, Cherfils J, Jackson CL (1999) Brefeldin A acts to stabilize an abortive ARF-GDP-Sec7 domain protein complex: involvement of specific residues of the Sec7 domain. *Mol Cell* **3:** 275–285

Pfanner N, Glick BS, Arden SR, Rothman JE (1990) Fatty acylation promotes fusion of transport vesicles with Golgi cisternae. *J Cell Biol* **110:** 955–961

Pfanner N, Orci L, Glick BS, Amherdt M, Arden SR, Malhotra V, Rothman JE (1989) Fatty acyl-coenzyme A is required for budding of transport vesicles from Golgi cisternae. *Cell* **59:** 95–102

Pham NTK, Khamrin P, Nguyen TA, Kanti DS, Phan TG, Okitsu S, Ushijima H (2007) Isolation and molecular characterization of Aichi viruses from fecal specimens collected in Japan, Bangladesh, Thailand, and Vietnam. *J Clin Microbiol* **45:** 2287–2288

Reuter G, Boldizsár Á, Papp G, Pankovics P (2009) Detection of Aichi virus shedding in a child with enteric and extraintestinal symptoms in Hungary. *Arch Virol* **154:** 1529–1532

Rust RC, Landmann L, Gosert R, Tang BL, Hong WJ, Hauri HP, Egger D, Bienz K (2001) Cellular COPII proteins are involved in production of the vesicles that form the poliovirus replication complex. *J Virol* **75:** 9808–9818

Sasaki J, Kusuhara Y, Maeno Y, Kobayashi N, Yamashita T, Sakae K, Takeda N, Taniguchi K (2001) Construction of an infectious cDNA clone of Aichi virus (a new member of the family *Picornaviridae*) and mutational analysis of a stem-loop structure at the 5′ end of the genome. *J Virol* **75:** 8021–8030

Sasaki J, Nagashima S, Taniguchi K (2003) Aichi virus leader protein is involved in viral RNA replication and encapsidation. *J Virol* **77:** 10799–10807

Sasaki J, Taniguchi K (2003) The 5′-end sequence of the genome of Aichi virus, a picornavirus, contains an element critical for viral RNA encapsidation. *J Virol* **77:** 3542–3578

Sasaki J, Taniguchi K (2008) Aichi virus 2A protein is involved in viral RNA replication. *J Virol* **82:** 9765–9769

Sbodio JI, Hicks SW, Simon D, Machamer CE (2006) GCP60 preferentially interacts with a caspase-generated golgin-160 fragment. *J Biol Chem* **281:** 27924–27931

Sdiri-Loulizi K, Gharbi-Khélifi H, de Rougemont A, Slaheddine C, Sakly N, Ambert-Balay K, Hassine M, Neji Guédiche M, Aouni M, Pothier P (2008) Acute infantile gastroenteritis associated with human enteric viruses in Tunisia. *J Clin Microbiol* **46:** 1349–1355

Sohda M, Misumi Y, Fujiwara T, Nishioka M, Ikehara Y (1994) Molecular cloning and sequence analysis of a human 372-kDa protein localized in the Golgi complex. *Biochem Biophys Res Commun* **205:** 1399–1408

Sohda M, Misumi Y, Yamamoto A, Yano A, Nakamura N, Ikehara Y. (2001) Identification and characterization of a novel Golgi protein, GCP60, that interacts with the integral membrane protein giantin. *J Biol Chem* **276:** 45298–45306

Suhy DA, Giddings TH, Kirkegaard K (2000) Remodeling the endoplasmic reticulum by poliovirus infection and by individual viral proteins: an autophagy-like origin for virus-induced vesicles. *J Virol* **74:** 8953–8965

Teterina NL, Gorbalenya AE, Egger D, Bienz K, Ehrenfeld E (1997) Poliovirus 2C protein determinants of membrane binding and rearrangements in mammalian cells. *J Virol* **71:** 8962–8972

Towner JS, Ho TV, Semler BL (1996) Determinants of membrane association for poliovirus protein 3AB. *J Biol Chem* **271:** 26810–26818

Wessels E, Duijsings D, Lanke KHW, van Dooren SHJ, Jackson CL, Melchers WJG, van Kuppeveld FJM (2006a) Effects of picornavirus 3A proteins on protein transport and GBF1-dependent COP-I recruitment. *J Viol* **80:** 11852–11860

Wessels E, Duijsings D, Niu TK, Neumann S, Oorschot VM, de Lange F, Lanke KHW, Klumperman J, Henke A, Jackson CL, Melchers WJG, van Kuppeveld FJM (2006b) A viral protein that blocks Arf1-mediated COP-I recruitment by inhibiting the guanine nucleotide exchange factor GBF1. *Dev Cell* **11:** 191–201

Yamashita T, Kobayashi S, Sakae K, Nakata S, Chiba S, Ishihara Y, Isomura S (1991) Isolation of cytopathic small round viruses with BS-C-1 cells from patients with gastroenteritis. *J Infect Dis* **164:** 954–957

Yamashita T, Sakae K, Kobayashi S, Ishihara Y, Miyake T, Mubina A, Isomura S (1995) Isolation of cytopathic small round virus (Aichi virus) from Pakistani children and Japanese travelers from Southeast Asia. *Microbiol Immunol* **39:** 433–435

Yamashita T, Sakae K, Tsuzuki H, Suzuki Y, Ishikawa N, Takeda N, Miyamura T, Yamazaki S (1998) Complete nucleotide sequence and genetic organization of Aichi virus, a distinct member of the *Picornaviridae* associated with acute gastroenteritis in humans. *J Virol* **72:** 8408–8412

Yamashita T, Sugiyama M, Tsuzuki H, Sakae K, Suzuki Y, Miyazaki Y (2000) Application of a reverse transcription-PCR for identification and differentiation of Aichi virus, a new member of the Picornavirus family associated with gastroenteritis in humans. *J Clin Microbiol* **38:** 2955–2961

Yang S, Zhang W, Shen Q, Yang Z, Zhu J, Cui L, Hua X (2009) Aichi virus strains in children with gastroenteritis, China. *Emerg Infect Dis* **15:** 1703–1705

Zhou Y, Atkins JB, Rompani SB, Bancescu DL, Petersen PH, Tang H, Zou K, Stewart SB, Zhong W (2007) The mammalian Golgi regulates Numb signaling in asymmetric cell division by releasing ACBD3 during mitosis. *Cell* **129:** 163–178

